General Disclaimer

One or more of the Following Statements may affect this Document

- This document has been reproduced from the best copy furnished by the organizational source. It is being released in the interest of making available as much information as possible.

- This document may contain data, which exceeds the sheet parameters. It was furnished in this condition by the organizational source and is the best copy available.

- This document may contain tone-on-tone or color graphs, charts and/or pictures, which have been reproduced in black and white.

- This document is paginated as submitted by the original source.

- Portions of this document are not fully legible due to the historical nature of some of the material. However, it is the best reproduction available from the original submission.

NASA TECHNICAL MEMORANDUM

NASA TM-73885

NASA TM-73885

THERMAL ENVIRONMENT EFFECTS ON STRENGTH AND IMPACT PROPERTIES OF BORON-ALUMINUM COMPOSITES

by H. H. Grimes and R. A. Lad
Lewis Research Center
Cleveland, Ohio

and

J. E. Maisel
Cleveland State University
Cleveland, Ohio

TECHNICAL PAPER to be presented at the
Second International Conference on Composite Materials
sponsored by the American Institute of Mining,
Metallurgical and Petroleum Engineers
Toronto, Canada, April 16-20, 1978

THERMAL ENVIRONMENT EFFECTS ON STRENGTH AND IMPACT PROPERTIES OF BORON-ALUMINUM COMPOSITES

H. H. Grimes, R. A. Lad, and J. E. Maisel*
National Aeronautics and Space Administration
Lewis Research Center
Cleveland, Ohio 44135

The understanding of the mechanism of thermally induced degradation in fracture properties of boron-aluminum composites could lead to increased use-temperatures of these important structural materials. To this purpose, we have systematically studied thermal effects on fracture strength and impact energy in 50 volume percent unidirectional composites of 143 and 203 μm boron fibers in 6061 and 1100 aluminum matrices. The room temperature effects of both cyclic (1500 and 3000 cycles) and static thermal histories were measured. For 6061 matrix composites, strength was maintained to approximately 400° C in the cyclic tests and higher than 400° C in the static tests. For the 1100 matrix composites, strength degradation appeared near 260° C after cycling and higher than 260° C in static heating. This composite strength degradation is explained by a fiber degradation mechanism resulting from a boron-aluminum interface reaction which produces a highly flawed fiber surface. The impact energy absorption degraded significantly only above 400° C for both matrix alloys. Thus, while impact loss for the 6061 composite correlates with the fiber strength loss, other energy absorption processes appear to extend the impact resistance of the 1100 matrix composites to temperatures beyond where its strength is degraded. Interrupted impact tests on as-received and thermally cycled composites define the range of load over which the fibers break in the impact event. Results of these tests confirm the relative role fiber strength plays in impact failure.

E-9498

*Cleveland State University.

STAR Category 24

Introduction

The maximum use-temperature of metal-matrix composites in static or cyclic temperature environments is often determined by the thermal degradation of their mechanical properties. Understanding of the thermal degradation mechanisms will provide insights which could extend the use capabilities of these materials. To this purpose, we have systematically studied at room temperature the degradation of fracture strength and impact energy in commercial B-Al composites in both static and cyclic thermal environments. In addition to the usual tensile and impact tests to define the onset and extent of the degradation, special interrupted impact testing and chemical dissolution of failed composites were used to acquire information which would lead to the understanding of the failure mechanisms. Electron and light microscopy and electron diffraction analysis provided additional definition of the degradation processes.

Materials

The composites used in this study were fabricated by TRW, Inc. from either 143 μm (5.6 mil) or 203 μm (8 mil) boron on tungsten fiber supplied by Avco Systems Division. These composites contained approximately 50 vol percent boron fibers, unidirectionally aligned in either a 6061 Al or 1100 Al matrix.

Initial vacuum bonding parameter studies were conducted for 0.5 hours at 34 MN/m^2 pressure and temperatures of 450°, 480°, and 510° C. From miniaturized Izod impact tests, it was determined that for the specimens bonded at 450° C, that maximum impact energy absorption could be achieved while still maintaining an adequate fiber/matrix bond. Based on this, all further vacuum bonded test materials were fabricated at 450° C.

In addition, a second group of composite panels was prepared using "air bonding" techniques (1). All subsequent testing that compared the composites prepared by these two techniques showed no differences in their properties either in the as-received state or after thermal treatment. This finding should provide additional confidence in the newer and faster "air bonding" technique.

All composite panels contained eight fiber plies. The average panel thickness for the 203 μm B composites was about 0.2 cm and about 0.14 cm for the 143 μm B composites. Tensile test coupons 1.1 by 10 cm, and impact test coupons 0.635 by 3.81 cm were cut from these panels so that the fibers were aligned parallel to the long axis of the coupon. Exact specimen size measurements were made and used in all mechanical testing.

Experimental

Thermal cycling of both the tensile and impact test coupons was done by alternately dipping a frame supporting the coupons into a hot fluidized sand bath at the test temperature and then into a similar cold bath that equilibrated near 50° C. The thermal cycle consisted of a 2.7 minute hot period and a 1.2 minute cold period as described in an earlier paper (2).

Static thermal environment for other coupons was provided by simple furnace heating in air for times equivalent to the time at maximum temperature for the 3000 cycle tests.

After cycling to the desired number of cycles or heating for the desired time at temperature, doublers were attached to the ends of the tensile coupons with a contact adhesive. Room temperature longitudinal tensile strengths were obtained with an Instron machine using wedge type grips. A crosshead speed of 0.126 cm/min was used in all tests.

All impact testing was done on the miniaturized coupon specimens in an Izod mode. These miniaturized specimens were failed at room temperature in a Tinus-Olsen Model 66 Impact Tester in which the tup was fitted with strain gages that permitted load-time and energy-time display and recording. In the normal test, the specimen extended as a cantilevered bar 2.54 cm from the vise and was struck by the tup at a distance 0.32 cm from the free end. The initial velocity of the hammer was 346 cm/sec. The 50 inch-pound range scale was used throughout to insure minimal velocity loss during impact while maintaining optimum sensitivity.

In order to study the failure processes early in the impact event (before complete fiber breakage), a special test was devised in which the specimen loading was interrupted prematurely. A lower range scale test could not be used because under these conditions, the initial velocity would be reduced and allowed to go to zero during the test. It was found that the premature unloading could be achieved without significant velocity degradation by providing that the tup would slip off the specimen end during deflection of the beam (Figure 1). Variation could be achieved by careful adjustment of the distance from vice to specimen free end. It should be noted, however, that the bending moment arm as determined by the vise to tup distance always remained constant.

After many of the tensile and normal impact tests and all of the interrupted impact tests, the aluminum matrix was removed by acid dissolution to expose the fibers. The fibers and fragments were then measured and counted to obtain the number and length distribution of broken fibers. Some fibers removed from tensile specimens were themselves pulled to failure to determine any strength loss due to thermal treatment. The acid (50 vol percent concentrated HCl in H_2O) apparently removed, in addition to the aluminum matrix, any interface reaction product formed during the thermal treatment (3). This permitted study of the fiber strength independent of the interface phase Microscopy and interface analyses were done as described in reference 2.

Results and Discussion

Tensile Strength

The tensile strengths of the composites after 3000 thermal cycles as a function of upper cycle temperature are shown in Figures 2, 3, 4, and 5. The curve, faired through the average values of the data points shown, conforms with that expected of a thermally activated flaw growth mechanism. Also shown in Figures 2, 3, 4, and 5 are bands which include all of the strength data for similar composites which have been held at 420° C for 135 hours, a time equivalent to the time-at-temperature for the 3000 cycle tests.

The temperature at which the strength of 6061 Al matrix, B-Al composites were significantly degraded after 3000 cycles was noticeably higher than that for the 1100 Al matrix composites. The 143 μm B-6061 Al composites maintained their as-received strength (plotted at 25° C) to above 400° C (Figure 2). In contrast, the 143 μm B-1100 Al composites show some degradation at temperatures as low as 260° C, with a gradual decrease to only one-third

of the as-received strength at 460° C (Figure 3). An approach to a lower limiting strength is indicated, which probably reflects a complete loss of fiber reinforcement and an approach to matrix properties.

The same general result is found for the 203 μm B fiber composites (Figures 4 and 5). The temperature at which degradation appears in the 203 μm B-6061 Al composites is somewhat less certain because of wider scatter in the data at 360° C. However, for the 203 μm B-1100 Al composites, the thermal degradation follows the 143 μm composite degradation almost exactly.

Static heating at 420° C resulted in no significant strength degradation for the 6061 Al matrix composites with either size fiber. Both 1100 matrix composites did show some degradation at 420° C but markedly less than those cycled to 420° C. This result is consistent with previous findings of reference 2 which illustrated the dependence of the degradation mechanism on thermal cycle deformation. The enhanced degradation due to static heating of the 1100 Al matrix composite compared with the 6061 matrix composite is again noted.

The mechanisms of composite strength degradation based on boron fiber strength degradation resulting from fiber-matrix interfacial reactions reported earlier for Avco composites (2) seems applicable here as well. Arguments given in this earlier paper led to a strength degradation mechanism based on the premature failure of highly flawed fibers resulting from fiber/matrix reactions. Figures 6 and 7 show strength data from reference 2 for fibers removed from 203 μm B-Al composites cycled 3000 times to 320° and 420° C. Each data point represents the average strength value of usually six fibers removed from a specific composite specimen. The roughened boron fiber surfaces observed by scanning electron microscopy were attributed to the nonuniform interface reaction of Al and B promoted by the thermal stress-induced breakdown of the interface protective oxide layers. Based on limited electron diffraction of the interface zone, the reaction thought responsible for the degradation was the formation of AlB_2. It now appears likely, based on the different appearance of the fiber surfaces from 1100 and 6061 Al matrix materials cycled 3000 times to 420° C (Fig. 8), and from private communications with A. Lawley and M. Koczak from Drexel University, that the interface reactions are not the same for the two alloys. This may contribute to the differences we observed in the temperatures at which strength degradation appears for the two alloys. While the observed morphological and compositional differences do not explain the nature of the difference in degradation mechanism, nevertheless, it is significant that the choice of matrix alloy may be of unexpected importance in controlling the onset of thermal degradation of tensile strength.

Impact Energy

The effect of thermal history on impact properties is indicated in Figures 9, 10, 11, and 12. Shown as a function of upper cycle temperature are the ratios of impact energy absorbed to failure of thermally cycled composites to that for as-received specimens (IE_T/IE_{AR}). Data for specimens tested at 1500 and 3000 cycles are given. The averages of the as-received impact energies measured were 55 KJ/m^2 for the 143 μm B-6061 Al composite, 49 KJ/m^2 for 143 μm B-1100 Al, 94 KJ/m^2 for 203 μm B-6061 Al and 111 KJ/m^2 for the 203 μm B-1100 Al composite. The absolute impact energy values found were not plotted here since these numbers would be of little engineering value because of the strong dependence of these on test geometry (4) and the nonstandard tests used here. Normalization of the data, however, does permit direct comparison of the impact data to the tensile strength degradation data previously shown in Figures 2, 3, 4, and 5. The normalized strength

(UTS_T/UTS_{AR}) curves obtained from these data are as shown in Figures 9, 10, 11, and 12 as solid lines.

The most noticeable difference between the impact energy and tensile strength data is the temperature at which thermal degradation appears. For all four composites studied, no degradation of the impact energy absorption appeared much below 400° C. Contrast this with the tensile strength curves for 143 μm B-1100 Al and 203 μm B-1100 Al composites where degradation appeared as low as 260° C.

Reduction of fiber strength after thermal treatment was found to be critical in composite tensile strength results. For impact energy absorption, other factors such as matrix and interface properties assume greater importance. For these properties, thermal treatment may act in a way to actually increase their impact energy absorption capability, compensating for the loss due to fiber strength degradation. Such increases in impact energy are indeed seen in the figures for composites cycled to 320° and 420° C. However, no trend with fiber size or matrix material was noted. In general, the energy degradation did not appear to be very cycle dependent either; that is, the effect of 1500 cycles was much the same as that for 3000 cycles.

To learn more of the role of fiber failure during the impact failure event a special interrupted impact test was devised. This test was described in the Experimental section.

Figure 13 shows typical load-time curves for 203 μm B-1100 Al and for 203 μm B-6061 Al composites which have been struck close to the specimen end. The curves lettered a, b, and c are for interrupted tests in which all fibers were not failed. Curve d represents the load time behavior when the fibers have just all failed. Curves a, b, c, and d are obtained as progressively more of the specimen extends beyond the tup. In the "standard" test used to obtain the data of Figures 9, 10, 11, and 12, enough of the specimen extended beyond the tup so that all the fibers broke before the tup cleared the specimen.

From the load-time curves for the interrupted tests, it is possible to plot the number of unbroken fibers versus maximum load. Such a plot is shown in Figure 14 for 203 μm B-6061 Al and 203 μm B-1100 Al composites. The number of unbroken fibers is determined by actual count after matrix dissolution. Data are shown for (a) as-received composites and (b) specimens cycled 1500 times to 460° C, a temperature at which the fibers are clearly degraded in strength.

One can obtain from Figure 14 the load required to break the first fiber and the minimum load required to fail all of the fibers. For the 6061 matrix as-received composite, the fibers are all broken over a narrow range of load, whereas for the 1100 matrix composite, the load range required to break all the fibers is considerably higher. This increase probably results from the unloading of the fibers by increased shear deformation possible in the softer 1100 matrix. Breaking of the last fibers only occurs after greater deflection of the B-1100 Al composite beam. This increased deflection contributes to increase the energy absorption on impact for this composite.

The effect of thermal cycling to 460° C is presented in Figure 14b. The general behavior shown for the as-received material is also seen for the thermally cycled material, except that the load to failure is less than half of that for the as-received values. This is consistent with the thermally induced fiber strength degradation model. The impact energy losses shown in Figures 11 and 12 also correlate very well with the strength losses of Fig-

ures 4 and 5. It appears, then, that for this relatively high temperature treatment, the impact energy loss is due primarily to fiber strength degradation. However, at somewhat lower temperatures, matrix and perhaps interface effects may contribute strongly to impact strength retention even though the tensile strength results indicate a fiber degradation. This was seen also in the normal impact tests for the 1100 Al matrix composites where the capacity to absorb impact energy was maintained or even increased at these temperatures.

Clearly, all of the energy absorption processes have not been investigated completely to fully establish their role in the thermal degradation process, nor has the role of fiber fracturing been completely defined. Some factors currently under investigation at our laboratory include; the effects of multiple fiber fracturing, exactly when in the impact event the fibers have fractured, and how time dependent are these processes.

References

1. Prewo, K. M., "Exploratory Development on Low Cost Primary Fabrication Processes for Boron-Aluminum Composites," AFML TR-74-40, AD-783293, Mar. 1974.

2. Grimes, H. H., Lad, R. A., and Maisel, J. E., "Thermal Degradation of the Tensile Strength of Unidirectional Boron-Aluminum Composites," Metallurgical Transactions A, Vol. 8 A, No. 12, Dec. 1977.

3. Greenwood, N. N., Parish, R. V., and Thornton, P., "Metal Borides," Quarterly Review (London), Vol. 20, No. 3, 1966, pp. 441-464.

4. Prewo, K. M., "Development of Impact Resistant Metal Matrix Composites," AFML TR-75-216, AD-A030800, Sept. 1975.

List of Figures

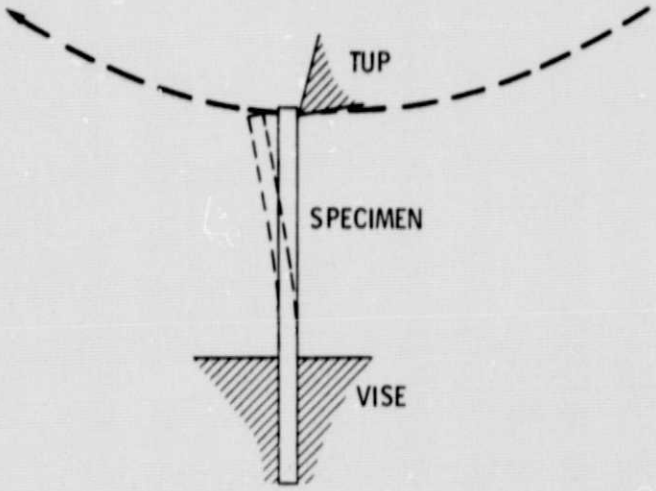

Figure 1. - Modified Izod impact test geometry to achieve premature unloading of the specimen.

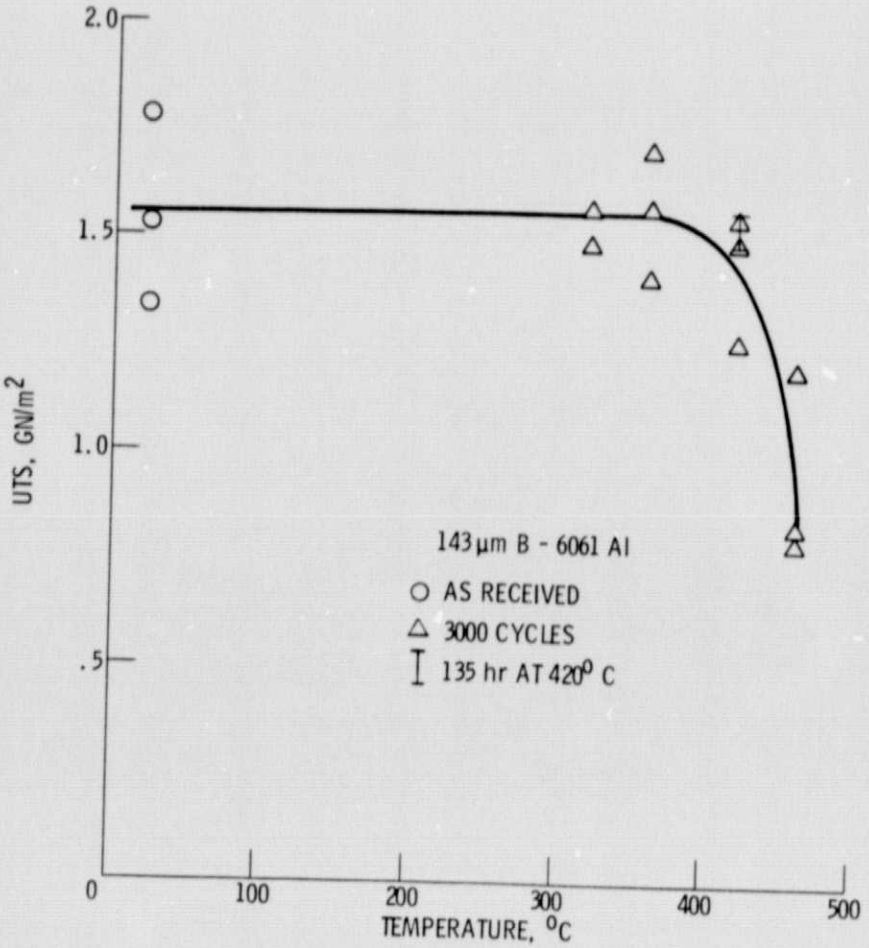

Figure 2. - Room temperature ultimate tensile strengths of 143 μm B-6161 Al matrix composites cycled 3000 times to indicated temperatures. Range of strengths of similar composites annealed at 420^0 C is also shown.

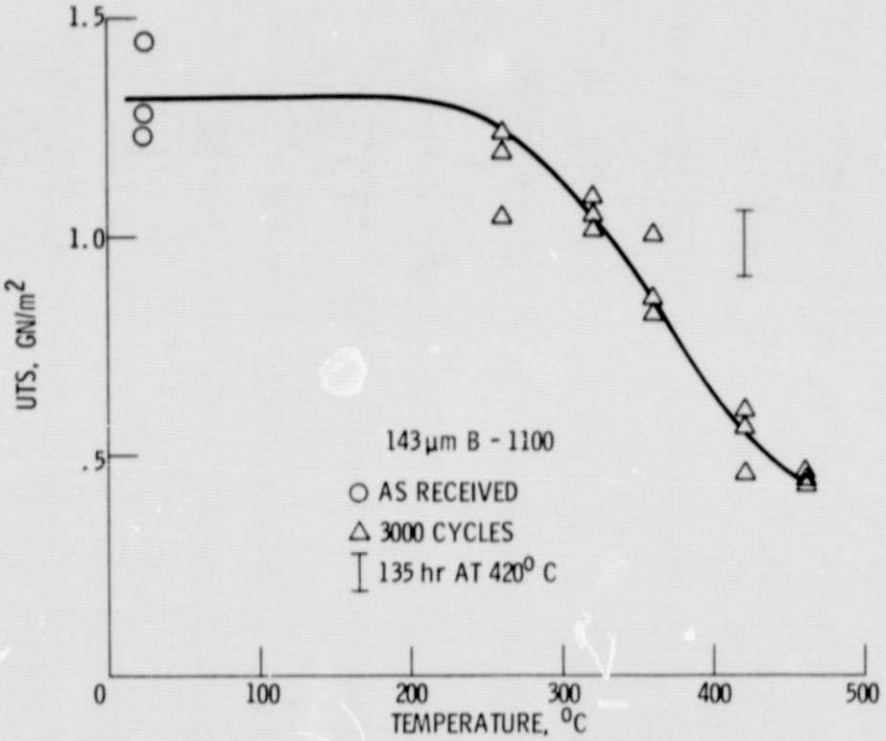

Figure 3. - Room temperature ultimate tensile strengths of 143 µm B-1100Al matrix composites cycled 3000 times to indicated temperatures. Range of strengths of similar composites annealed at 420^0 C is also shown.

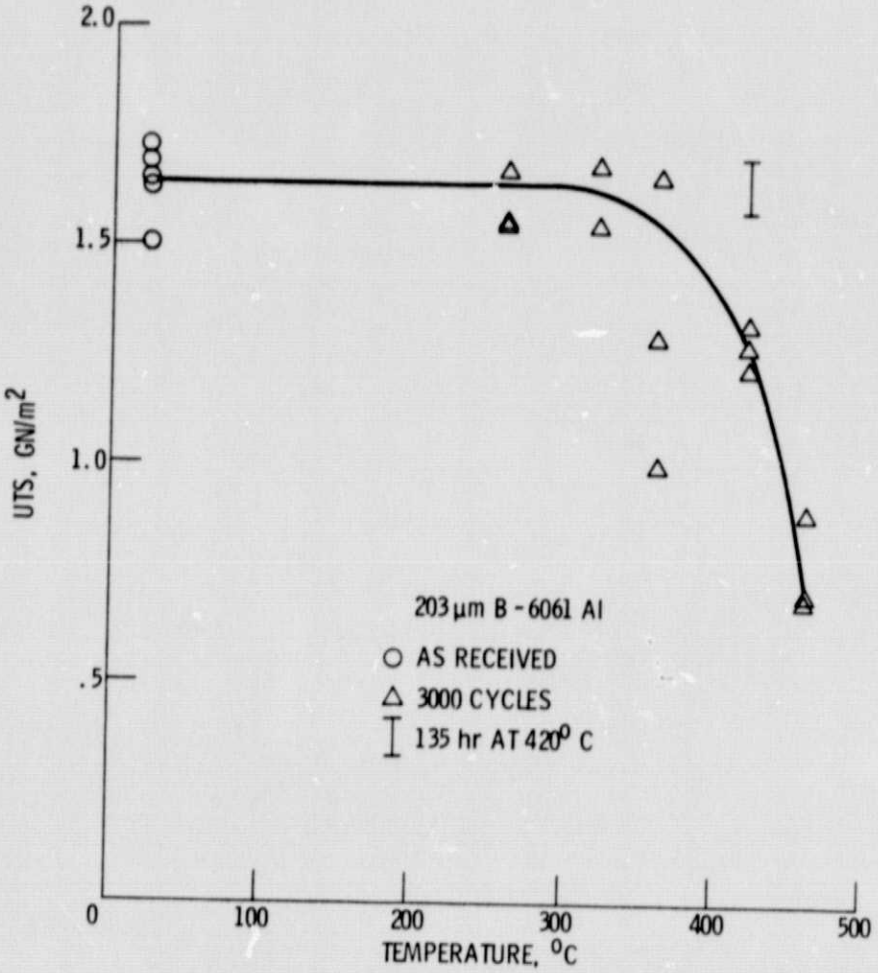

Figure 4. - Room temperature ultimate tensile strengths of 203 μm B-6061 Al matrix composites cycled 3000 times to indicated temperatures. Range of strengths of similar composites annealed at 420^0 C is also shown.

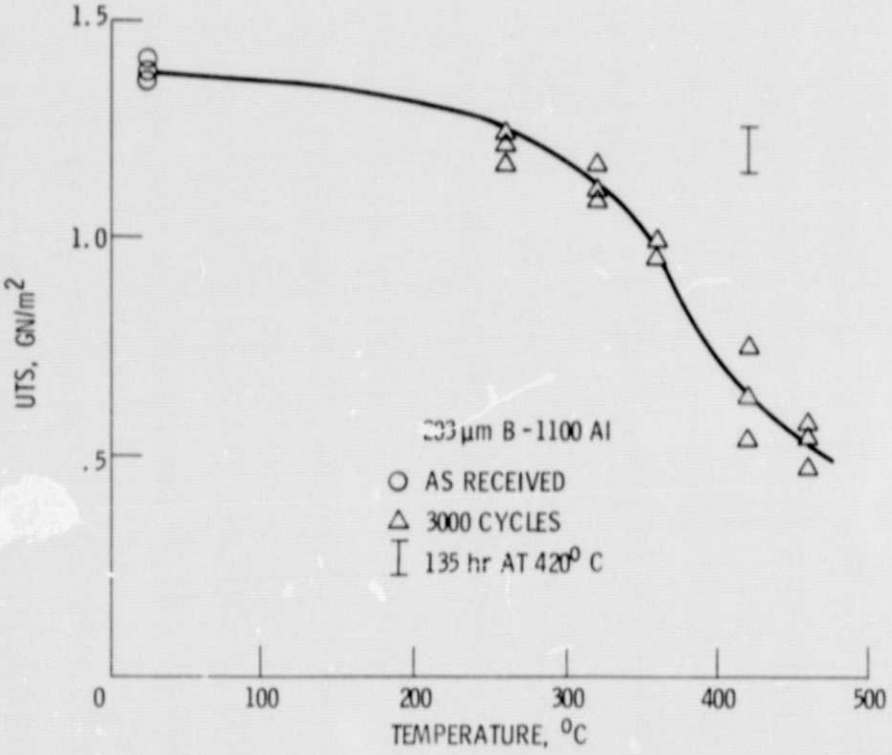

Figure 5. - Room temperature ultimate tensile strengths of 203 μm B-1100 Al matrix composites cycled 3000 times to indicated temperatures. Range of strengths of similar composites annealed at 420° C is also shown.

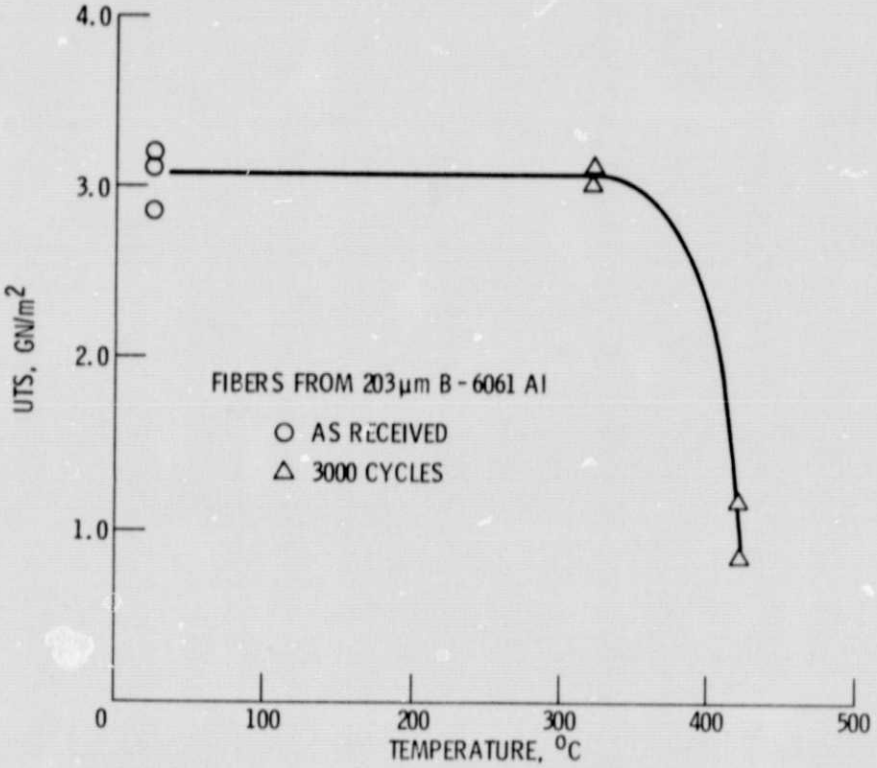

Figure 6. - Room temperature ultimate tensile strengths of fibers removed from 203μm B-6061 Al composites cycled 3000 times to indicated temperatures. (From ref. 2.)

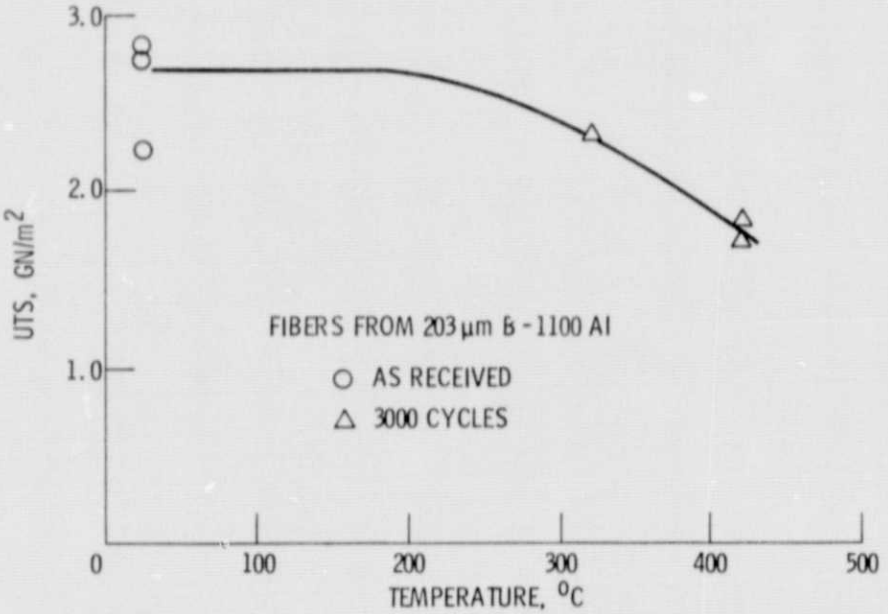

Figure 7. - Room temperature ultimate tensile strengths of fibers removed from 203 μm B-1100 Al matrix composites cycled 3000 times to indicated temperatures. (From ref. 2.)

E-3418

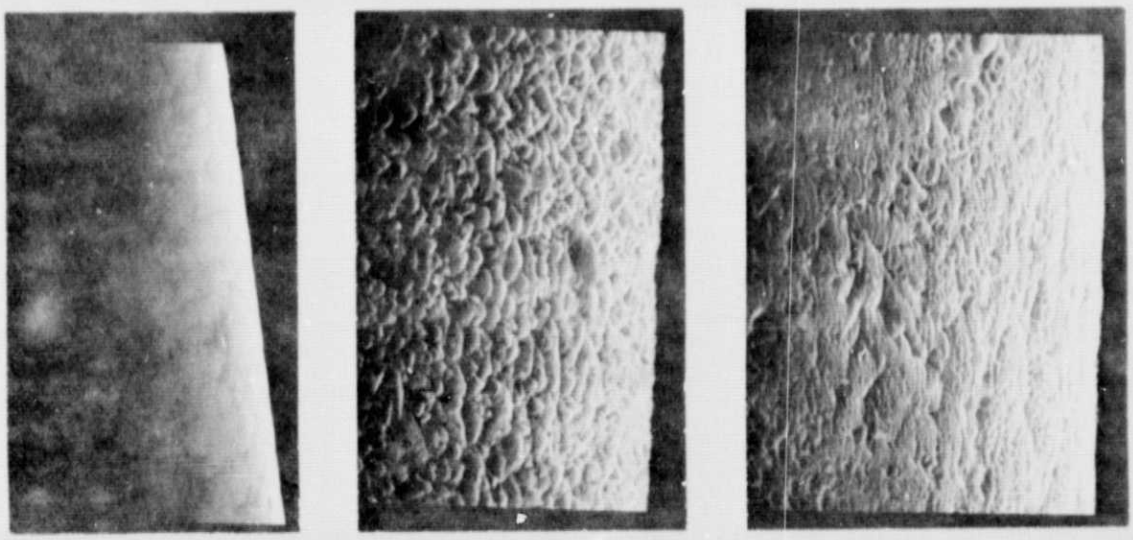

AS-RECEIVED 6061 1100

Figure 8. - Scanning electron micrograph of the surfaces of fibers removed from 203 μm B-1100 Al and 203 μm B-6061 composites after 3000 cycles to 420^0 C. An as-received fiber surface is shown for comparison, X1500.

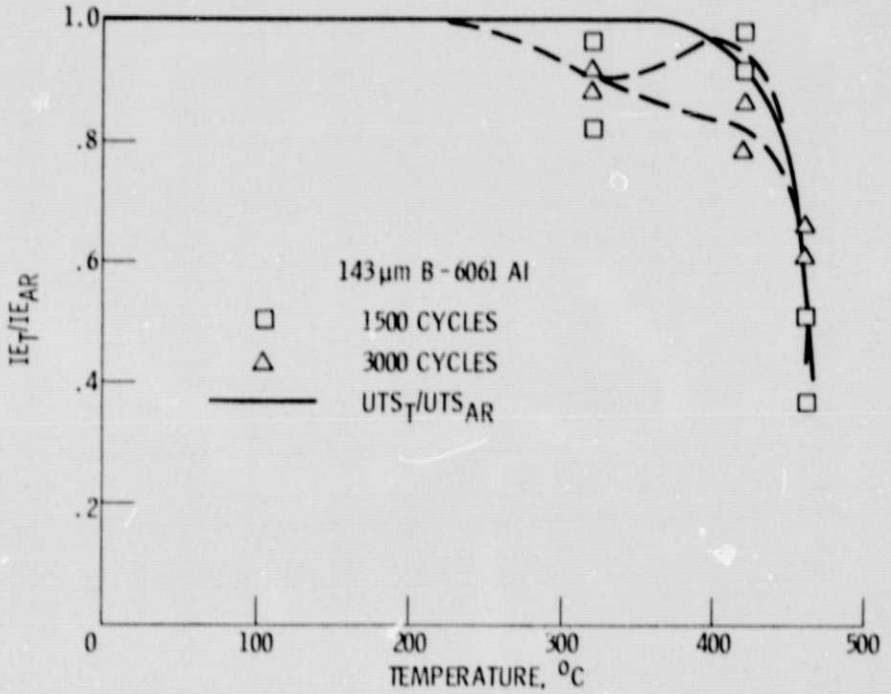

Figure 9. - Ratios of impact energies of thermally cycled 143 μm B-6061 Al composites to the average impact energies of as-received composites as a function of upper cycle temperature. Corresponding ultimate tensile strength ratios are also shown.

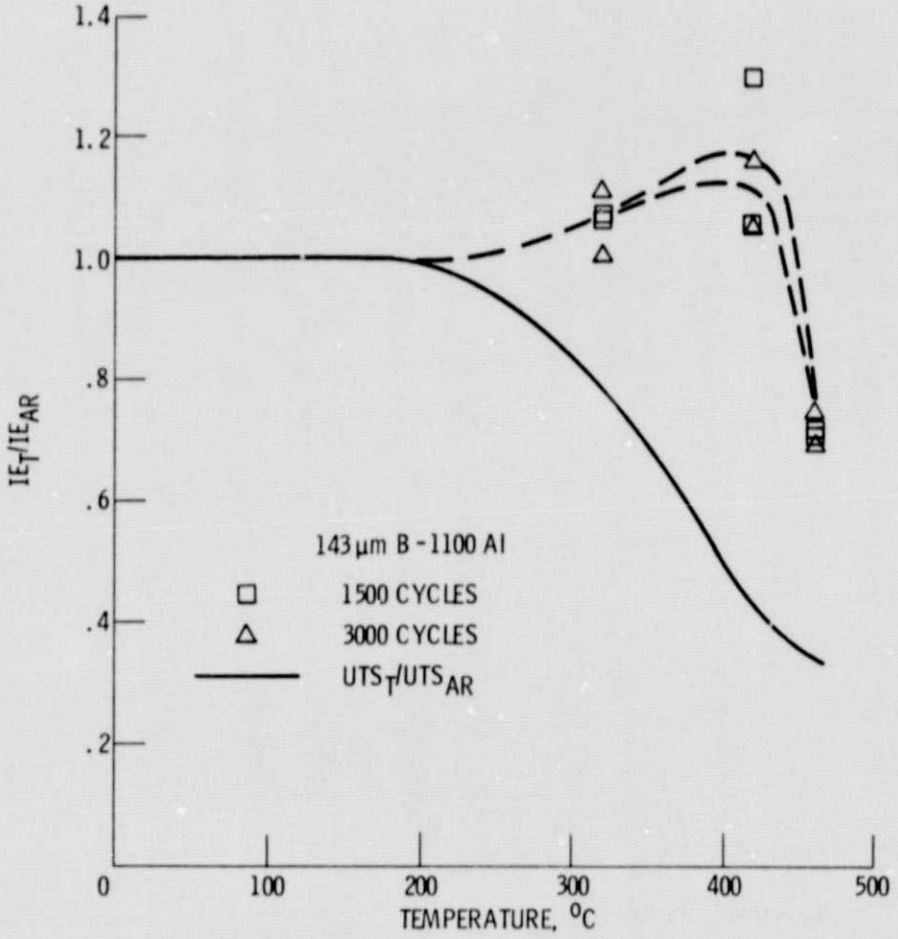

Figure 10. - Ratios of impact energies of thermally cycled 143μm B-1100 Al composites to the average impact energies of as-received composites as a function of upper cycle temperature. Corresponding ultimate tensile strength ratios are also shown.

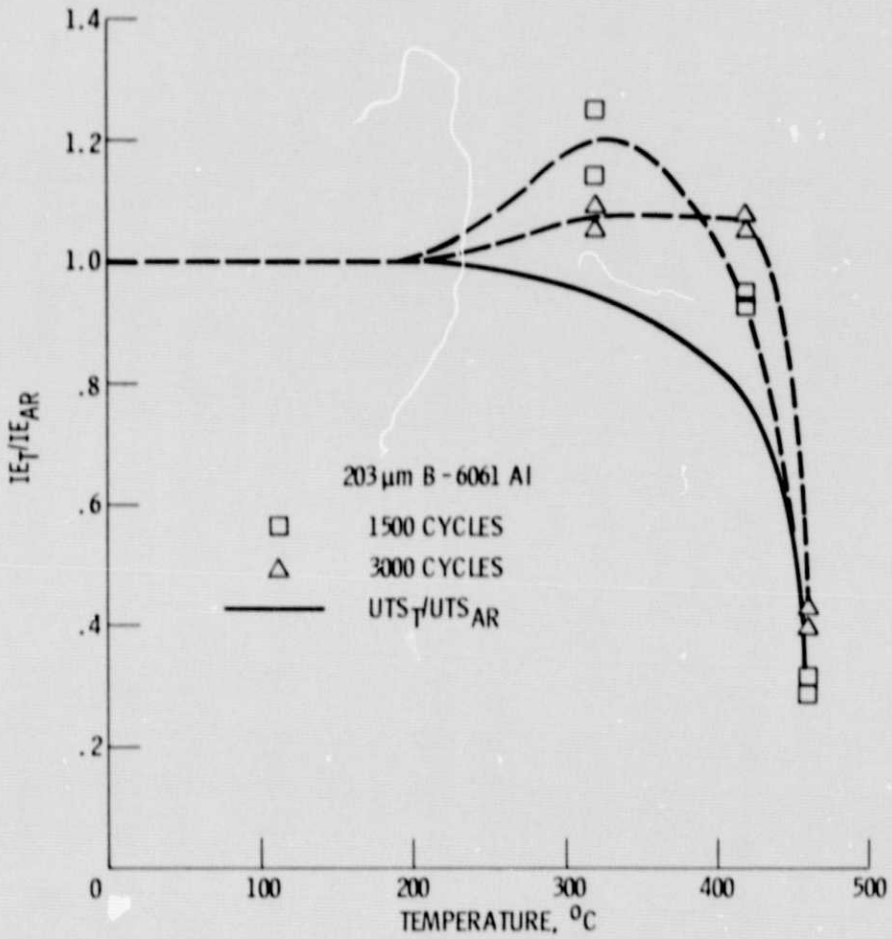

Figure 11. - Ratios of impact energies of thermally cycled 203 μm B-6061 Al composites to the average impact energies of as-received composites as a function of upper cycle temperature. Corresponding ultimate tensile strength ratios are also shown.

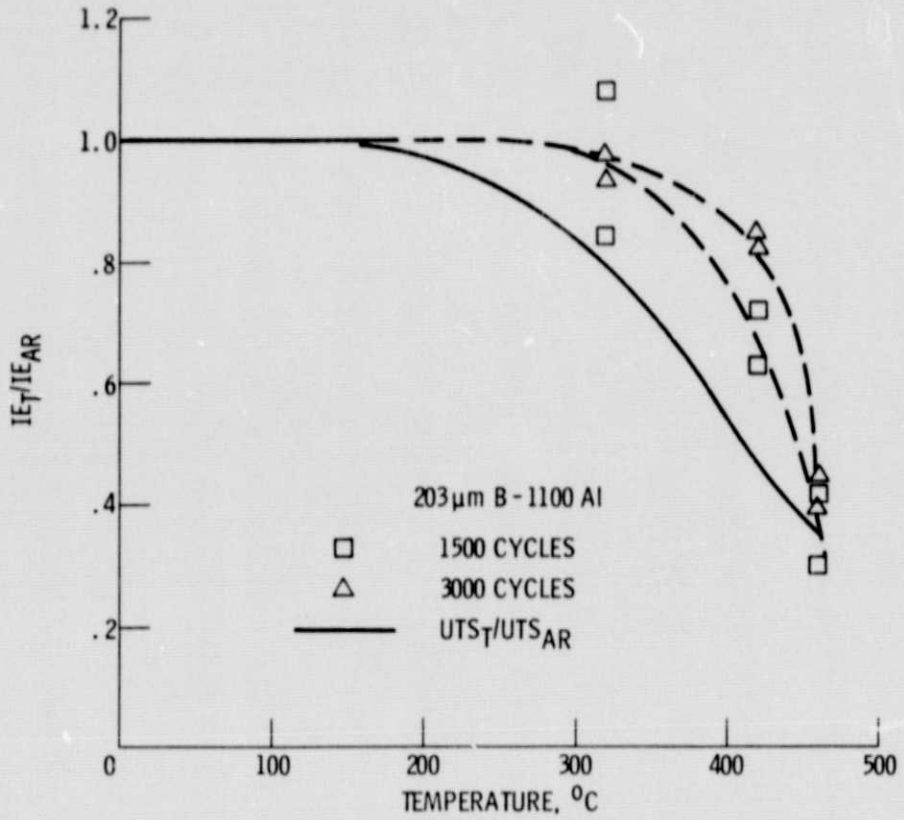

Figure 12. - Ratios of impact energies of thermally cycled 203μm B-1100 Al composites to the average impact energies of as-received composites as a function of upper cycle temperature. Corresponding ultimate tensile strength ratios are also shown.

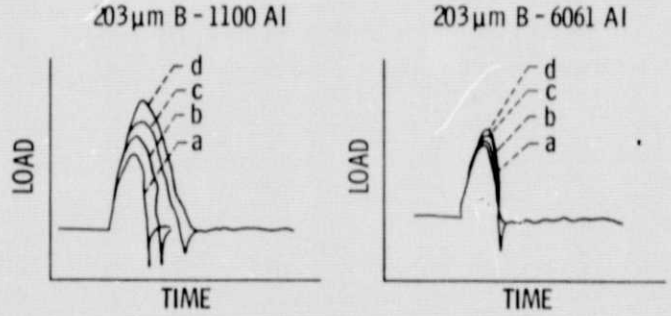

Figure 13. - Load-time curves for 203μm B-1100 Al and 203μm B-6061 Al composites for progressively longer loading periods before interruption.

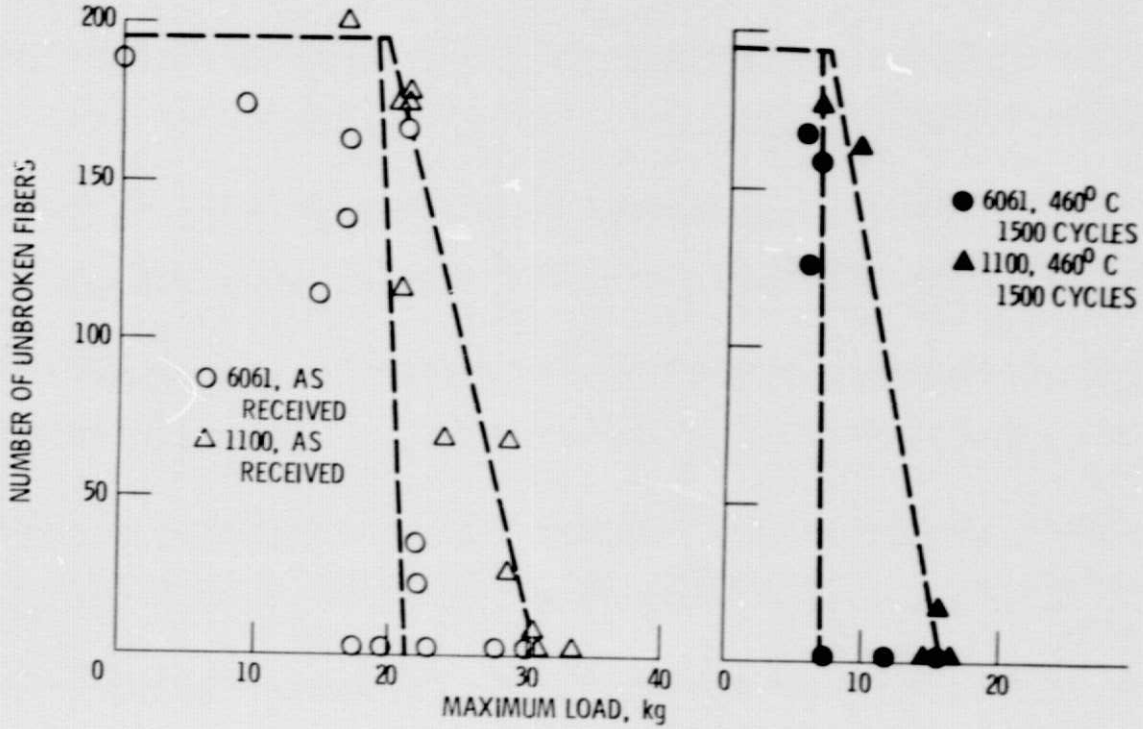

(a) OPEN SYMBOLS ARE FOR AS-RECEIVED COMPOSITES.

(b) CLOSED SYMBOLS FOR COMPOSITES CYCLED 1500 TIMES TO 460° C.

Figure 14. - Numbers of unbroken fibers remaining after interrupted impacts of 203 μm B-6061 Al and 203 μm B-1100 Al composites versus maximum impact load.